

Optimum Index Profile of the Perfluorinated Polymer-Based GI Polymer Optical Fiber and Its Dispersion Properties

Takaaki Ishigure, Yasuhiro Koike, and James W. Fleming, *Member, OSA*

Abstract—The significant advantages in bandwidth and low material dispersion of perfluorinated (PF) polymer-based graded-index polymer optical fiber (GI POF) are theoretically and experimentally reported for the first time. It is confirmed that the low attenuation and low material dispersion of the PF polymer enables 1 Gb/s km and 10 Gb/s km transmission at 0.85- μm and 1.3- μm wavelengths, respectively. The PF polymer-based GI POF has very low material dispersion (0.0055 ns/nm \cdot km at 0.85 μm), compared with those of the conventional PMMA-based POF and of multimode silica fiber (0.0084 ns/nm \cdot km at 0.85 μm). Since the PF polymer-based GI POF has low attenuation from the visible to near infrared region, not only the 0.65- μm wavelength which is in the low attenuation window of the PMMA-based GI POF, but other wavelengths such as 0.85- μm or 1.3- μm etc. can be adopted for the transmission wavelength. It is clarified in this paper that the wavelength dependence of the optimum index profile shape of the PF polymer-based GI POF is very small, compared to the optimum index profile shape of the silica-based multimode fiber. As a result, the PF polymer-based GI POF has greater tolerance in index profile variation for higher speed transmission than multimode silica fiber. The impulse response function of the PF polymer-based GI POF was accurately analyzed from the measured refractive index profile using a Wentzel, Kramers, Brillouin (WKB) numerical computation method. By considering all dispersion factors involving the profile dispersion, predicted bandwidth characteristic of the PF polymer-based GI POF agreed well with that experimentally measured.

Index Terms— Graded-index polymer optical fiber (GI POF), material dispersion, perfluorinated polymer, profile dispersion.

I. INTRODUCTION

GROWING research interest has been focused on the development of optical components and devices that have the capability to support high-speed multimedia networks. Silica-based single-mode optical fiber is widely utilized in the long distance trunk area for the order of giga bit per second transmission because of its high bandwidth and transparency. Use of silica-based multimode fiber is a recent trend in the area of local area network (LAN) and interconnection. The large core diameter of the silica-based multimode fiber, for example, 50

and 62.5 μm , relaxes the tolerance required for connection compared to the single mode fiber that has typical core diameter of only 5 to 10 μm . However, even in the multimode silica fiber, accurate alignment using a ferrule in the connector is still required.

We have proposed a large-core, high-bandwidth, and low-loss graded index polymer optical fiber (GI POF) [1], [2] as an alternative to the silica multimode fiber. The large core (200–1000 μm) of the GI POF enables the use of inexpensive polymer connectors without ferrules. These can be prepared by an injection molding process, because a slight amount of displacement such as ± 30 μm in the connection does not seriously influence the coupling loss. Further, a core of 100 μm or more could virtually eliminate the serious modal noise, which exists in the multimode silica fibers [3].

Poly (methyl methacrylate) (PMMA) has been generally used as the core material of commercially available step-index type POF, and its attenuation limit is approximately 100 dB/km at the visible region [4]. The high attenuation of POF compared to silica-based fiber has limited the POF data link length, even if the bandwidth characteristics are improved by GI POF.

The development of the perfluorinated (PF) amorphous polymer-based GI POF [5], [6] opened the way for an improvement in the high-speed POF network. Since intrinsic absorption loss due to carbon-hydrogen stretching vibrations that exist in PMMA-based POF is completely eliminated in the PF polymer-based POF, the experimental total attenuation of the PF polymer-based GI POF decreases to 40 dB/km even in the near infrared region.

The PF polymer has smaller material dispersion than that of silica or PMMA. It is confirmed that the maximum bandwidth is approximately 10 GHz km if the refractive index profile is optimized. Optimization of the index profile of the PF polymer-based GI POF is also discussed in this paper for the first time.

II. DISPERSION OF PF POLYMER-BASED GI POF

A. Material Dispersion

We have already reported [7] that the material dispersion, which is induced by the wavelength dependence of the refractive index of the polymer and the finite spectral width of the light source, strongly affects the dispersion properties in the case of the PMMA-based GI POF. It is also indicated that [7] substitution of fluorine atoms for hydrogen atoms decreases not

Manuscript received July 30, 1999; revised October 28, 1999. This work is supported by the research fund of Plastic Optical Fiber Project from Telecommunications Advancement Organization (TAO) of Japan.

T. Ishigure and Y. Koike are with the Keio University, Faculty of Science and Technology, Yokohama 223-8522, Japan. They are also with the Kanagawa Academy of Science and Technology, Yokohama 236-0004, Japan.

J. W. Fleming is with the Lucent Technologies, Bell Labs, Murray Hill, NJ 07974 USA.

Publisher Item Identifier S 0733-8724(00)01320-7.

only the intrinsic absorption loss but also the material dispersion. Therefore, it is an important issue to investigate the material dispersion of the PF polymer to design the high-speed PF polymer-based GI POF link.

The material dispersion of the PF polymer-based GI POF was evaluated by measuring the wavelength dependence of the refractive index of a PF polymer bulk specimen. The material dispersion was estimated by (1) [8]

$$D_{\text{mat}} = - \left(\frac{\lambda \delta_{\lambda}}{c} \right) \left(\frac{d^2 n}{d\lambda^2} \right) L \quad (1)$$

where δ_{λ} is the root mean square spectral width of the light source, λ the wavelength of transmitted light, c the velocity of light, $d^2 n/d\lambda^2$ the second derivative of the refractive index with respect to wavelength, and L is the length of fiber. The refractive index data as a function of wavelength was fit to a three term Sellmeier equation to calculate $d^2 n/d\lambda^2$ in (1).

B. Dispersion Induced by the Refractive Index Profile

In order to discuss the total dispersion of the GI POF, the power-law form described by (2) approximated the refractive index profile of the GI POF

$$n(r) = \begin{cases} n_1 \left[1 - 2\Delta \left(\frac{r}{a} \right)^g \right]^{1/2} & 0 \leq r \leq a \\ n_2 & r \geq a \end{cases} \quad (2)$$

where, n_1 and n_2 are the refractive indexes of the core center and cladding respectively, a is the core radius, and Δ is the relative index difference defined by

$$\Delta = \frac{n_1^2 - n_2^2}{2n_1^2}. \quad (3)$$

The parameter g called index exponent determines the refractive index profile. The index exponents of various kinds of GI POF's prepared in our laboratory were estimated by approximating the measured index profile using a least-squares fit of (2). An analytical solution of Maxwell's wave equation can be obtained by means of Wentzel, Kramers, Brillouin (WKB) method. The obtained analytical solution of the wave equation enables calculation of the impulse response function width. Details of the calculation method are described in [7] and [8]. Finally, the total dispersion of the PF polymer-based GI POF was estimated for the first time, by considering the material dispersion and the dispersion induced by the refractive index profile.

III. RESULTS AND DISCUSSION

A. Material Dispersion

Experimental results of refractive index measurements of PF homopolymer, the PF dopant added PF polymer and PMMA are shown in Fig. 1 compared with those of pure silica and GeO₂ doped silica reported in [8], in which the solid lines are the approximated result from the fitted Sellmeier equations. The prism coupling by using METRICON prism coupling refractive index measurement system measured the refractive index of the polymer. The apparatus of the refractive index measurement utilizing the prism coupling method has a great advantage that it is possible to measure the refractive index of

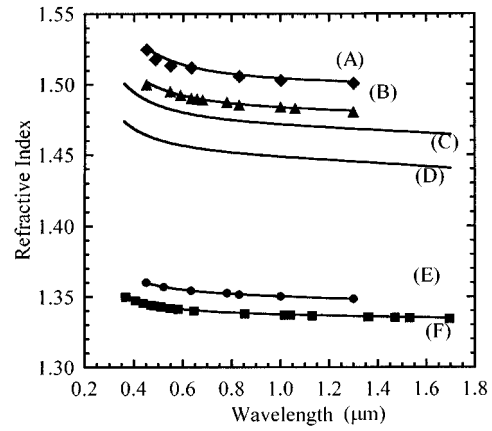


Fig. 1. Wavelength dependence of the refractive indexes of PMMA, PF polymer and silica. (A): 15 wt.% benzyl benzoate (BEN) added PMMA; (B): PMMA homopolymer; (C): 13.5 mol% GeO₂-doped SiO₂; (D): pure SiO₂. (E): 5.5 wt.% PF dopant added PF polymer; (F): PF homopolymer. Plots: experimentally measured results. Solid line: approximated by Sellmeier equation.

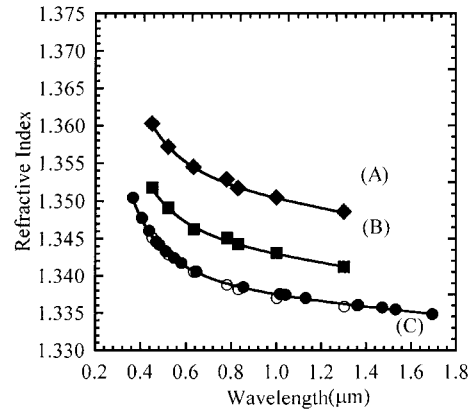


Fig. 2. Wavelength dependence of the refractive indexes of PF dopant added PF polymer and PF homopolymer. Solid line: approximated by Sellmeier equation. (A) 5.5-wt.% PF dopant added PF polymer. (B) 2.5 wt.% PF dopant added PF polymer. (C) PF homopolymer. •: measured by minimum deviation method ◊, ◼: measured by prism coupling method.

bulk sample with high accuracy. Since only the polymer sample having one polished face is required for the measurement, the preparation process of the sample becomes simple. In order to evaluate the degree of measurement error, the refractive index of the PF polymer was also measured by the autocollimation method [8]–[10]. For this autocollimation method, the prism like sample is required, which is similar to the minimum deviation method. In this method, one face of the prism is given a reflecting surface. The prism is systematically rotated but the angle of interest is that where the incident light is refracted, and once again refracted along the same trajectory as the incident beam. The results are indicated in Fig. 2. A good agreement is observed in the results measured by two different methods. Therefore, the prism coupling method, which is simpler, is adopted for the measurement of the refractive index in samples in this paper. The measured refractive index values were fitted to a three terms Sellmeier equation of the form

$$n^2 - 1 = \sum_{i=1}^3 \frac{A_i \lambda^2}{\lambda^2 - \ell_i^2} \quad (4)$$

where n is the refractive index of polymer sample, A_i is the oscillator strength, l_i is the oscillator wavelength, and λ is the wavelength of light. The linear least squares fitting routine based on the Levenberg–Marquard method was used. The fitting routine requires that starting values be supplied for the parameter. The starting values used in this investigation were those estimated from pure silica. In the case of polymers in this paper, the Sellmeier model provides the best fit for data when two of the oscillators are in the ultraviolet (UV) and one is in the infrared, which is the same as in silica. The mean residual is $\approx 1 \times 10^{-4}$. The material dispersion of the PF polymer estimated by (1) is shown in Fig. 3 compared to those of PMMA and silica. The material dispersion of the PF polymer is smaller than that of the silica particularly in the visible to near infrared region. Since the material dispersion decreases with increasing wavelength as indicated in Fig. 3, the operating wavelength of the POF network could be in the near infrared region rather than in the visible region for high-speed data transmission. The 0.65- μm wavelength has been selected for the conventional PMMA-based POF network so far, because the low attenuation window is located at 0.65 μm .

Fig. 4 shows the experimental result of the attenuation spectrum of the PF polymer-based GI POF compared to that of the PMMA-based GI POF. In the PMMA-based GI POF, the attenuation abruptly increases in longer wavelength than 0.7 μm , which is due to the intrinsic absorption loss of the carbon-hydrogen stretching vibration. Such absorption peaks are eliminated in the spectrum of PF polymer-based GI POF. The minimum attenuation of the PF polymer-based GI POF was 40 dB/km from 1.0 to 1.3- μm wavelength. Low attenuation at near infrared region is advantageous even with the dispersion limitation because the material dispersion decreases with increasing wavelength, as mentioned above. The values of the material dispersions of PF polymer, dopant added PF polymer, pure silica, and GeO₂-doped silica at 0.65, 0.85, and 1.3- μm wavelengths are summarized in Table I. The material dispersion of PF polymer at 0.65- μm wavelength is 0.13 ns/nm km which is much lower than that (0.32 ns/nm km) of the PMMA at the same wavelength. Further, the material dispersions of the PF polymer at 0.85 and 1.3- μm wavelengths decrease to 0.054 and 0.009 ns/nm km, respectively.

Although the material dispersion of silica is almost zero at 1.3- μm wavelength, the high material dispersion of the GeO₂ doped silica from visible to near infrared region limits the bandwidth of GeO₂–SiO₂-based fiber. On the other hand, it is noteworthy that addition of dopant in the PF polymer causes little change in value of material dispersion. Since perfluorinated substance is used as the dopant, the material dispersion of the dopant is low. Furthermore, the material dispersion of PF homopolymer is almost the same as that of dopant added PF polymer in the wavelength range from 0.45 to 1.3 μm , which indicates that the higher bandwidth PF polymer-based GI POF is expected from the visible to the near infrared region.

B. Dispersion Induced by Refractive Index Profile

Total dispersion is estimated by using WKB method, considering material, modal and profile dispersions, as described in detail in this section. Approximation of power-law index profile in

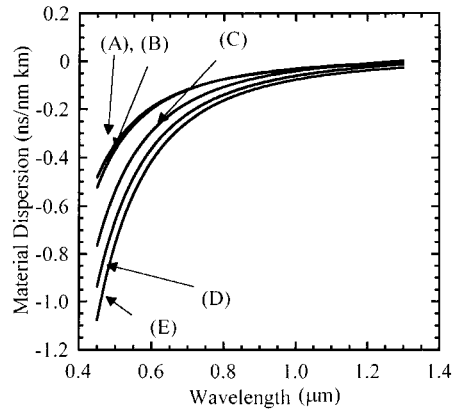


Fig. 3. Material dispersion of PMMA, PF polymer and silica. (A) PF homopolymer. (B) 15 wt.% PF dopant added PF polymer. (C) pure SiO₂. (D): 13.5 mol% GeO₂-doped SiO₂. (E): PMMA homopolymer.

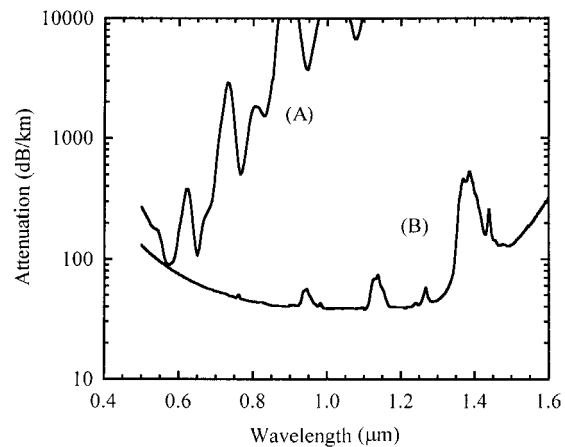


Fig. 4. Total attenuation spectra of PMMA-based and PF polymer-based GI POF. (A) PMMA-based GI POF and (B) PF polymer-based GI POF.

TABLE I
MATERIAL DISPERSION OF PF POLYMER
AND SILICA

	PF polymer		Silica	
	dopant added	homopolymer	GeO ₂ added	pure SiO ₂
0.65 μm	0.1294	0.1318	0.2792	0.2227
0.85 μm	0.0524	0.05476	0.1118	0.0838
1.3 μm	0.00567	0.00900	0.01178	0.00272
	ns/nm · km			

(2) enabled calculation of the root-mean-square (rms) width σ of the impulse response of GI POF as a function of index exponent g by the WKB method [7], [8], [11]. Subsequently, the relation between the refractive index profile and the bandwidth of the GI POF was obtained by using the simple relation between the width of impulse response and the bandwidth as shown in (5)

$$f_{-3\text{dB}} = \sqrt{\frac{\ln 2}{2\pi^2}} \frac{1}{\sigma} = \frac{0.188}{\sigma} \quad (5)$$

where σ is the root mean square width of the impulse response function calculated. Here, -3 dB bandwidth of the GI POF was calculated by assuming that the output pulse waveform was approximated by Gaussian shape. For comparison, the calculated

data of PMMA-based GI POF and GeO₂-SiO₂-based multimode glass fiber are also shown in Fig. 5 in which it is assumed that the source spectral width is 3 nm.

The maximum bandwidth of the PMMA-based GI POF at 0.65- μm wavelength is limited to approximately 3 GHz for 100 m by the large material dispersion. It is noteworthy that in the case of silica-based multimode glass fiber, the maximum bandwidth (approximately 2 GHz for 100 m) at 0.65- μm wavelength is almost the same as or lower than that of PMMA-based GI POF, although the bandwidth more than 40 GHz can be achieved when the signal wavelength is 1.3 μm . On the other hand, the small material dispersion of the PF polymer-based GI POF permits the maximum bandwidth higher than 5 GHz even at 0.65 μm . Furthermore, when the signal wavelength is 1.3 μm , theoretical maximum bandwidth achieves to 80 GHz for 100 m, which is even higher than that of silica-based multimode fiber at the same wavelength. The difference of the maximum bandwidth between the PF polymer-based GI POF and the silica-based multimode fiber is mainly caused by the difference between the material dispersion of dopant-doped PF polymer and GeO₂-doped silica.

It should be noted that the difference of the optimum index exponent value between 0.65 and 1.3- μm wavelengths is caused by the inherent polarization properties of material itself. The optimum index profile of the GI fiber for maximum bandwidth is described by (6) when the index profile is approximated by the power-law equation shown in (2) [11]

$$g_{\text{opt}} = 2 - \frac{2n_1}{N_1} \cdot P - \Delta \frac{\left(4 - \frac{2n_1}{N_1} \cdot P\right) \left(3 - \frac{2n_1}{N_1} \cdot P\right)}{5 - \frac{4n_1}{N_1} \cdot P} \quad (6)$$

$$N_1 = n_1 - \lambda \frac{dn_1}{d\lambda} \quad (7)$$

where g_{opt} signifies the optimum index exponent, and P that is called as profile dispersion is written as follows:

$$P = \frac{\lambda}{\Delta} \frac{d\Delta}{d\lambda}. \quad (8)$$

Since the profile dispersion P is the function of the differentiation of the relative index difference Δ with respect to wavelength λ , the optimum index profile depends on refractive index of the core material, which means that index increment by the dopant material is a key issue. The wavelength dependence of the bandwidth characteristics of PF polymer-based GI POF is shown in Fig. 6, compared to that of the GeO₂-SiO₂-based multimode glass fiber when the index profile is controlled to have the index exponents of 2.03, 2.075, and 2.23 in the PF polymer-based GI POF, and 2.01 and 1.78 in the silica-based multimode fiber. Selected index exponents of 2.03, 2.07 and 2.23 are the optimum index exponents of the PF polymer-based GI POF when the source wavelengths are 0.65, 0.85 and 1.3 μm , respectively, while 2.01 and 1.78 are optimum for 0.85 and 1.3- μm wavelength, respectively, in the silica-based multimode fiber. It is indicated in Fig. 6 that if the index exponent g is controlled to around 2.0, several hundreds MHz km can be achieved in wide wavelength range from 0.6 to 1.3 μm , because

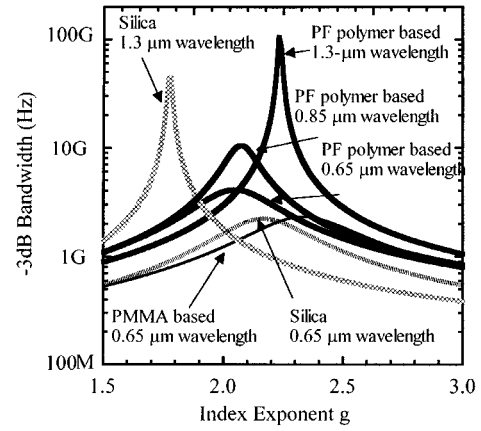


Fig. 5. Relation between the index exponent g and the bandwidth of 100 m PMMA-based, PF polymer-based GI POF's and GeO₂-SiO₂-based GI glass fiber.

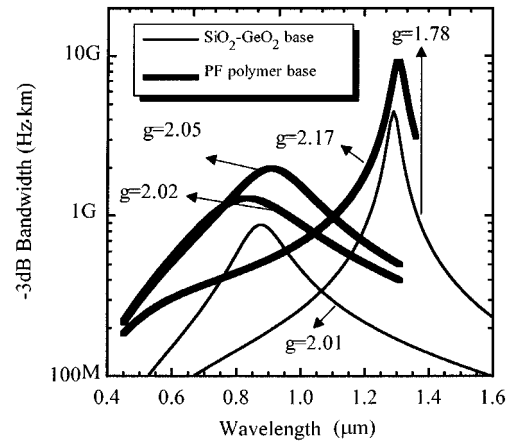


Fig. 6. Wavelength dependence of the bandwidth of PF polymer-based GI POF and GeO₂-SiO₂-based GI multimode glass fiber.

of low material dispersion. On the other hand, in the case of the SiO₂-GeO₂-based GI multimode fiber, accurate index profile control for specified wavelength of used laser is necessary to achieve several hundreds MHz/km, since the wavelength dependence of the bandwidth is much stronger than that of the PF polymer as shown in Fig. 6. It can be emphasized that the low material dispersion of PF polymer allows the tolerance in the index profile of the PF polymer-based GI POF even for higher speed transmission than silica fiber.

For 1.3- μm use, the optimum index exponent g_{opt} is 2.23, by which approximately 10 GHz \cdot km can be achieved, while the same GI POF having 2.23 of index exponent exhibits only 400 MHz \cdot km when the wavelength of the light source is 0.65 μm . In order to further decrease the wavelength dependence of the optimum index profile, a suitable dopant, which can decrease the profile dispersion, i.e., the wavelength dependence of the relative index difference [see (8)] should be selected. The shift of the optimum index exponent of the PF polymer-based GI POF between 0.85- μm and 1.3- μm wavelengths is 0.16 (from 2.07 to 2.23) which is smaller than that (0.23) of GeO₂-SiO₂-based GI multimode glass fiber (from 2.01 to 1.78). This is because the profile dispersion of the PF polymer-based GI POF is smaller than that of GeO₂-SiO₂-based GI multimode glass fiber.

C. Experimental Bandwidth Characteristics

The bandwidth characteristic of the PF polymer-based GI POF were experimentally measured by the time domain measurement method [2], in which the impulse response function was measured by the output pulse broadening from the fiber when a narrow pulse such as 50 ps was injected to the fiber. A pulse of 10 MHz from a laser diode was injected (N.A. = 0.3.) into the POF. A sampling head (model OOS-01, Hamamatsu Photonics Co.), detected the output pulse. As the light source, the laser diodes whose emitting wavelengths are 0.65 and 1.3 μm were used. Measured results of 100-m length PF polymer-based GI POF are shown in Fig. 7 compared with the result of 100 m SI type polymer clad silica fiber (SI PCF).

Although a slight distortion is observed in the leading part (left side threshold) of the output pulse in the PF polymer-based GI POF, the pulse width is much smaller than that of SI PCF. The refractive index profile of the measured GI POF is shown in Fig. 8. As shown, the profile exhibits a tail around the core-cladding boundary, which differs from the optimum index profile approximated by power-law equation. The index exponent g approximated from the index profile in Fig. 8 is 1.8, which results in 1.7 GHz for 100 m of bandwidth at 0.65- μm wavelength as shown in Fig. 5. However, the measured bandwidth was 1 GHz which was lower than expected bandwidth. Comparison of measured and calculated bandwidth based on (2) for the PF polymer-based GI POF is shown in Fig. 9 compared with those of PMMA-based GI POF. In the case of the PMMA-based GI POF, excellent agreement between measured and estimated values is observed, while the experimental data (open circle) of the PF polymer-based GI POF is much lower than the calculated curve. Such difference would be due to the deviation of index profile from the power-law profile as shown in Fig. 8.

In order to accurately evaluate the dispersion characteristic of the GI POF whose index profile is deviated from power-law approximation, a numerical computation method based on WKB method was adopted [11], [12]. In the computation procedure, the index profile was described by a ten term polynomial function of the distance r from the center axis of the fiber as shown in (9)

$$n(r) = n_1 \left[1 - 2 \cdot \Delta \cdot \left\{ A_{10} \cdot \left(\frac{r}{a} \right)^{10} + A_0 \cdot \left(\frac{r}{a} \right)^9 + \dots + A_2 \cdot \left(\frac{r}{a} \right)^2 + A_1 \cdot \left(\frac{r}{a} \right) \right\} \right]^{1/2} \quad (9)$$

where $A_{10}, A_9, \dots, A_2, A_1$ are constants independent of the wavelength of transmitting light. By investigating the approximation accuracy, it was found that the ten terms are enough to describe various refractive index profile of the PF polymer-based GI POF. In this numerical method, the group delay τ of the mode can be expressed as

$$\tau = \frac{L}{c} \frac{k}{\beta} \left\{ \left[\int_{r_1}^{r_2} \frac{n^2 + nk \, dn/dk}{R} dr \right] / \int_{r_1}^{r_2} \frac{dr}{R} \right\} \quad (10)$$

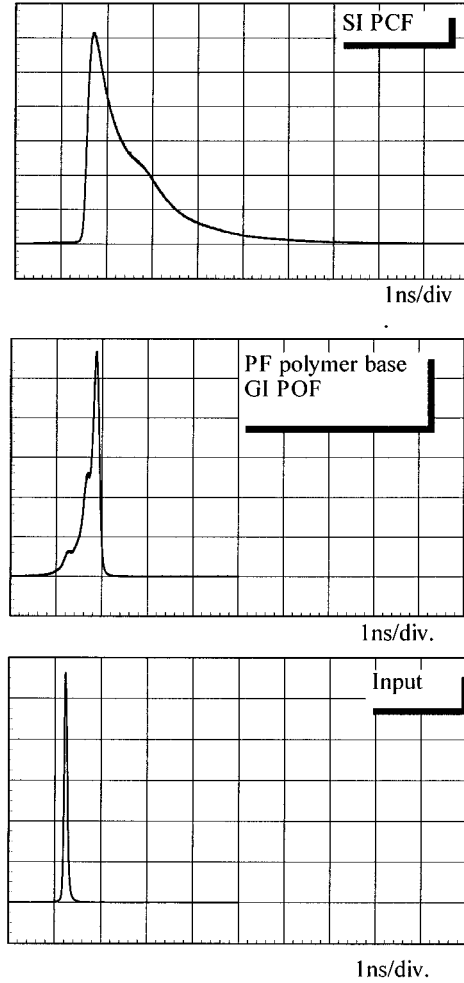


Fig. 7. Pulse broadening through 100 m PF polymer-based GI POF and step-index PCF at 0.65- μm wavelength.

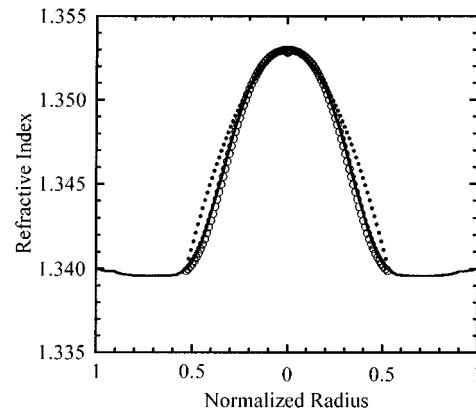


Fig. 8. Refractive index profile of the PF polymer-based GI POF. Solid line: measured index profile. \bullet : approximated index profile by power-law form when the index exponent g is 1.8. \circ : estimated index profile by ten terms polynomial fitting.

where, c, L , and β signify the light velocity in vacuum, fiber length and the propagation constant, respectively. The symbols k and R are written as

$$k = \frac{2\pi}{\lambda} \quad (11)$$

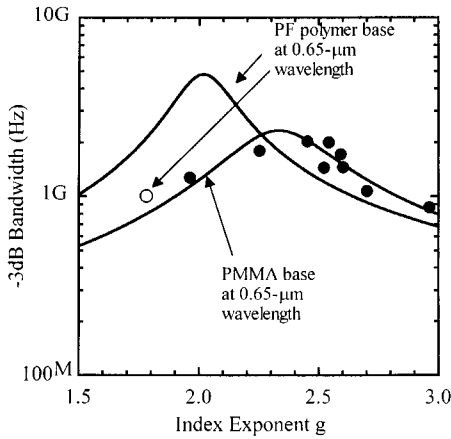


Fig. 9. Comparison between the measured and calculated bandwidth of the PF polymer-based and PMMA-based GI POF's at 0.65- μ m wavelength. \bullet : experimental data in PMMA-based GI POF. \circ : experimental data in PF polymer-based GI POF.

$$R = \sqrt{n(r)^2 k^2 - \beta^2 - \frac{\nu^2}{r^2}} \quad (12)$$

where ν is called the azimuthal mode number. In (10), the poles of r_1 and r_2 in the integrand are defined as the solutions of (13)

$$n(r)^2 k^2 - \beta^2 - \frac{\nu^2}{r^2} = 0. \quad (13)$$

After calculating the group delay τ of each mode, the time range between the group delay of the fastest and slowest mode was divided into 30 to 40 of time slots. The impulse response function was constructed by counting the number of modes whose group delay was involved in each time slot. The output waveform was calculated by the convolution of input pulse waveform and the impulse response function in which all modes were assumed to be equally excited.

The calculated result of the PF polymer-based GI POF whose index profile is shown in Fig. 8, is shown in Fig. 10 compared to experimentally measured data. The open circle in Fig. 10 is the calculated waveform by polynomial approximation, while the closed circle signifies the calculated waveform when the index profile is approximated by power-law form. When the index profile was approximated by polynomial form, the bandwidth estimated by the Fourier transform of the impulse response function was 1 GHz, which is exactly the same as the measured result in Fig. 9. It is noteworthy that an excellent agreement between the calculated and measured results can be achieved by the above procedure.

It was further confirmed from Figs. 8 and 10 that the leading part (left side threshold) of the output pulse in Fig. 10 is attributed to the tailing part of the index profile around the core-cladding boundary, in which higher modes arrived at the end of fiber earlier to form the above leading part of the output pulse. Such index profile deviation is improved by changing the fabrication process. By optimizing the refractive index profile of the PF polymer-based GI POF eliminating the tailing part

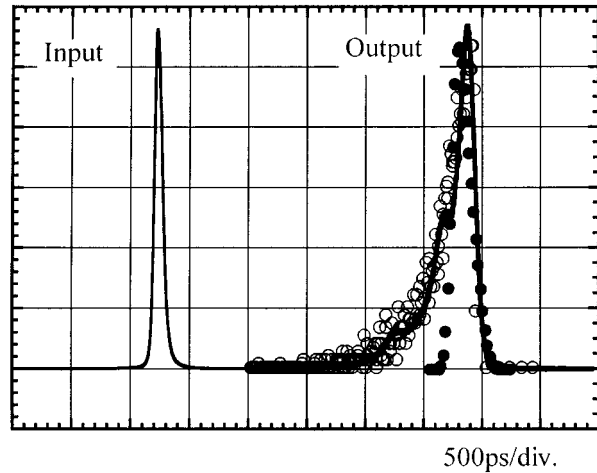


Fig. 10. Pulse broadening through 100 m PF polymer-based GI POF at 0.65- μ m wavelength. Solid line: measured waveform. \bullet : theoretically estimated output waveform when the index profile shown in Fig. 8 is estimated by power-law form when the index exponent g is 1.8. \circ : theoretically estimated output waveform when the index profile shown in Fig. 8 is estimated by ten terms polynomial fitting.

at the core-cladding boundary, higher bandwidth than conventional silica-based multimode fiber can be expected as shown in Figs. 5 and 6.

IV. CONCLUSION

Lower material dispersion of the PF polymer than PMMA and silica gives the great advantage in the bandwidth. It was reported for the first time that higher bandwidth than PMMA-based GI POF and GeO_2 - SiO_2 -based multimode fiber can be expected. Furthermore, low attenuation, which is another advantage of the PF polymer-based GI POF, enabled much higher bandwidth at 1.3 μ m because the material dispersion decreases with increasing the wavelength.

In order to theoretically confirm the high bandwidth of the PF polymer-based GI POF, the bandwidth characteristics were precisely analyzed with using WKB numerical computation method. Although the PF polymer has very low material dispersion, consideration of all the dispersion factors, particularly the profile dispersion enabled the precise prediction of bandwidth characteristics. The low attenuation (less than 40 dB/km from visible to near infrared region) and the low material dispersion of the PF polymer-based GI POF presents a solution to the ever-increasing bandwidth demand in access networks.

ACKNOWLEDGMENT

The authors wish to acknowledge N. Yoshihara, T. Tsukamoto, T. Ohnishi, and N. Naritomi for supplying materials and having many valuable discussions.

REFERENCES

- [1] R. E. Epworth, "The phenomenon of modal noise in analogue and digital optical fiber communication," in *Proc. 4th European Conf. Opt. Commun.*, Genoa, Italy, Sept. 1978, pp. 492-501.
- [2] Y. Koike, T. Ishigure, and E. Nihei, "High-bandwidth graded-index polymer optical fiber," *J. Lightwave Technol.*, vol. 13, pp. 1475-1489, July 1995.

- [3] T. Ishigure, E. Nihei, S. Yamazaki, K. Kobayashi, and Y. Koike, "2.5 Gb/s 100 m data transmission using graded index polymer optical fiber and high speed laser diode at 650-nm wavelength," *Electron. Lett.*, vol. 31, no. 6, pp. 467-468, 1995.
- [4] T. Kaino, M. Fujiki, and K. Jinguji, "Preparation of plastic optical fibers," *Rev. Electron. Commun. Lab.*, vol. 32, pp. 478-488, 1984.
- [5] Y. Koike and T. Ishigure, "Progress of low-loss GI polymer optical fiber from visible to 1.5- μ m wavelength," in *Proc. 23rd European Conf. Opt. Commun.*, vol. 1, Edinburgh, Scotland, Sept. 1997, pp. 59-62.
- [6] N. Yoshihara, "Low-loss, high-bandwidth fluorinated POF for visible to 1.3- μ m wavelength," in *Proc. Optic. Fiber Conf. (OFC'98)*, San Jose, CA, Feb. 1998, Paper ThM4.
- [7] T. Ishigure, E. Nihei, and Y. Koike, "Optimum refractive index profile of the grade-index polymer optical fiber, toward gigabit data links," *Appl. Opt.*, vol. 35, no. 12, pp. 2048-2053, 1996.
- [8] J. W. Fleming, "Material and mode dispersion in $\text{GeO}_2\text{-B}_2\text{O}_3\text{-SiO}_2$," *J. Amer. Cer. Soc.*, vol. 59, no. 11-12, pp. 503-507, 1976.
- [9] D. L. Wood and J. W. Fleming, Computerized refractive index measurement for fiber optic glasses, in NBS Special Publication #574, J. W. Feldman, Ed., vol. 91, 1980.
- [10] W. L. Bond, "Measurement of the refractive indices of several crystals," *J. Appl. Phys.*, vol. 36, no. 5, pp. 1674-1677, 1965.
- [11] R. Olshansky and D. B. Keck, "Pulse broadening in graded-index optical fibers," *Appl. Opt.*, vol. 15, no. 2, pp. 483-491, 1976.
- [12] D. Marcuse, "Calculation of bandwidth from index profiles of optical fibers. 1: Theory," *Appl. Opt.*, vol. 18, pp. 2073-2080, 1979.



Takaaki Ishigure was born in Gifu, Japan, on July 30, 1968. He received the B.S. degree in applied chemistry and the M. S. and Ph.D. degrees in material science from Keio University, Japan, in 1991, 1993, and 1996, respectively.

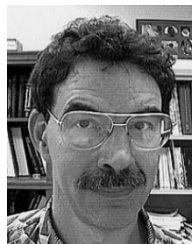
He is currently an Instructor of Keio University, Japan. His current research interest is in fabrication and system application of the graded-index polymer optical fiber.



Yasuhiro Koike was born in Nagano, Japan, on April 7, 1954. He received the B.S., M.S., and Ph.D. degrees in applied chemistry from Keio University, Japan, in 1977, 1979, and 1982, respectively.

He has been an Associate Professor of Keio University and developed the high-bandwidth GI polymer optical fiber. He has been concurrently the leader of "High-Speed POF" project of Kanagawa Academy of Science and Technology, Japan, since 1995. He stayed as a Visiting Researcher at AT&T Bell Laboratories from 1989 to 1990.

Dr. Koike received the International Engineering and Technology Award of the Society of Plastics Engineers in 1994.



James W. Fleming was born in St. Louis, MO, on May 23, 1947. He received the B.S. and M.S. degrees in ceramic engineering and science from the University of Missouri at Rolla in 1970 and 1971, respectively, and the Ph.D. degree in ceramic science and engineering from Rutgers University, NJ, in 1981.

He is currently a Distinguished Member of Technical Staff at Bell Laboratories, NJ, a Division of Lucent Technologies, where he has worked in optical fiber research for 25 years. He has published over 80 papers, holds 26 patents, and has authored two books

in this area of research. He is currently interested in optical fiber materials and processing.

Dr. Fleming has received several technical awards including the Distinguished Alumnus award from the Ceramic Engineering Department at the University of Missouri in 1984, and Fellow of the American Ceramic Society in 1989. He is a member of the Optical Society of America (OSA).